In Retinal Cones, Membrane Depolarization in Darkness Activates the cGMP-dependent Conductance

A Model of Ca Homeostasis and the Regulation of Guanylate Cyclase

JAMES L. MILLER and JUAN I. KORENBROT

From the Department of Physiology, School of Medicine, University of California at San Francisco, San Francisco, California 94143

ABSTRACT   We measured outer segment currents under voltage clamp in solitary, single cone photoreceptors isolated from the retina of striped bass. In darkness, changes in membrane voltage to values more positive than 10 mV activate a time- and voltage-dependent outward current in the outer segment. This dark, voltage-activated current (DVAC) increases in amplitude with a sigmoidal time course up to a steady-state value, reached in 0.75–1.5 s. DVAC is entirely suppressed by light, and its current–voltage characteristics and reversal potential are the same as those of the light-sensitive currents. DVAC, therefore, arises from the activation by voltage in the dark of the light-sensitive, cGMP-gated channels of the cone outer segment. Since these channels are not directly gated by voltage, we explain DVAC as arising from a voltage-dependent decrease in cytoplasmic Ca concentration that, in turn, activates only guanylate cyclase and results in net synthesis of cGMP. This explanation is supported by the finding that the Ca buffer BAPTA, loaded into the cytoplasm of the cone outer segment, blocks DVAC. To link a decrease in cytoplasmic Ca concentration to the synthesis of cGMP and the characteristics of DVAC, we develop a quantitative model that assumes cytoplasmic Ca concentration can be continuously calculated from the balance between passive Ca influx via the cGMP-gated channel and its active efflux via a Na/Ca,K exchanger, and that further assumes that guanylate cyclase is activated by decreasing cytoplasmic Ca concentration with characteristics identical to those described for the enzyme in rods. The model successfully simulates experimental data by adjusting the Ca conductance of the cGMP-gated channels as a function of voltage and the Ca buffering power of the cytoplasm. This success suggests that the activity of guanylate cyclase in cone outer segments is indistinguishable from that in rods.

Address correspondence to Dr. Juan I. Korenbrot, Department of Physiology, School of Medicine, Box 0444, University of California at San Francisco, San Francisco, CA 94143.

INTRODUCTION

Light suppresses the current that flows continuously in the dark across the plasma membrane of the outer segment in rod and cone photoreceptors of the vertebrate retina (for reviews see Pugh and Cobbs, 1986; McNaughton, 1990). The light-dependent decrease in current arises from the closure of ion channels gated by cytoplasmic cyclic GMP (cGMP) and located exclusively in the plasma membrane of the outer segment (for reviews see Yau and Baylor, 1989; Korenbrot and Maricq, 1991). Light decreases the concentration of cGMP by triggering the activation of a phosphodiesterase (PDE) that hydrolyzes the nucleotide (for reviews see Pugh and Cobbs, 1986; Liebman, Parker, and Dratz, 1987). With time, the cGMP concentration returns to its dark level as a result of the activity of a guanylate cyclase (for review see Pugh and Lamb, 1990). Illumination also lowers the cytoplasmic Ca concentration in the outer segment (McNaughton, Cervetto, and Nunn, 1986; Ratto, Payne, Owen, and Tsien, 1988). Ca concentration is maintained by a balance between a passive Ca influx, via the cGMP-gated channels, and an active efflux, via a Na/Ca,K exchanger located in the same membrane (Yau and Nakatani, 1985; Miller and Korenbrot, 1987). Light causes a decrease in Ca concentration because it reduces Ca influx (by closing the cGMP-gated channels) in the presence of the continuous, light-independent efflux. Recovery of Ca concentration to dark levels follows the reopening of the cGMP-gated channels (Miller and Korenbrot, 1987).

The precise magnitude and time course of the concentration changes of cGMP and Ca in either rods or cones remain to be determined. It is clear, however, that whereas cGMP directly controls the opening and closing of the plasma membrane channels (for review see Yau and Baylor, 1989), Ca acts as a modulator, controlling the light sensitivity and kinetics of the transduction signal (Korenbrot and Miller, 1986; Torre, Matthews, and Lamb, 1986). The role of Ca as a modulator is particularly apparent in the process of light adaptation: in light-adapted rods or cones, the transduction signal generated by a given flash is lower in sensitivity and faster in time course than in dark-adapted cells (for review see McNaughton, 1990). Light adaptation is compromised if Ca concentration changes are attenuated by cytoplasmic buffers (Korenbrot and Miller, 1986; Torre et al., 1986; Matthews, 1991) and does not occur if Ca concentration changes are prevented by manipulation of the solution bathing the cells (Nakatani and Yau, 1988; Fain, Lamb, Matthews, and Murphy, 1989; Matthews, Fain, Murphy, and Lamb, 1990).

The mechanisms that enable Ca to modulate cGMP concentration changes are now under investigation. In rods, biochemical (Fleischman and Denisevich, 1979; Lolley and Racz, 1982; Pepe, Boero, Vergani, Panfoli, and Cugnoli, 1986; Koch and Stryer, 1988) and electrophysiological (Kawamura and Murakami, 1989) experiments have demonstrated that guanylate cyclase activity is dependent on Ca over the concentration range expected in intact photoreceptors, between 10 nM and 1 µM. Comparable evidence is not available for cones. In rods, the velocity of guanylate cyclase increases cooperatively as the Ca concentration decreases. This increase is well described by a Hill equation with half-maximum activation at ~90 nM Ca and a power coefficient of 4 (Koch and Stryer, 1988). The Ca dependence of guanylate cyclase activity is independent of light and is mediated by a 26-kD Ca binding protein (Dizhoor, Ray,

Kumar, Niemi, Brolley, Spencer, Walsh, Philipov, Hurley, and Stryer, 1991; Lambrecht and Koch, 1991). The effects of Ca on PDE activity in rods are less clear. Recent electrophysiological experiments suggest that in nearly intact rods, the lifetime of the light-activated form of PDE, but not its maximum velocity, increases as the Ca concentration rises between 30 nM and 1 μM (Kawamura and Murakami, 1991). This regulation, too, is apparently mediated by a distinct Ca-binding protein of 26 kD molecular mass (Kawamura and Murakami, 1991). In contrast, biochemical studies of rod disk membranes have failed to demonstrate regulation of light-activated PDE over a comparable range of Ca concentrations, although interesting effects of Ca are observed in the nonphysiological range between 0.1 and 5 mM (Robinson, Kawamura, Abramson, and Bownds, 1980; Kawamura and Bownds, 1981; Del Priore and Lewis, 1983; Barkdoll, Pugh, and Sitaramayya, 1989). The potential regulation by Ca of PDE activity in cones has not been investigated.

Transduction signals in cone photoreceptors are faster in time course, lower in light sensitivity, and more robust in their adaptation features than those in rods (for review see Baylor, 1987; McNaughton, 1990). A detailed molecular explanation for these differences is not at hand. However, biochemical (Hurwitz, Bunt-Milam, Change, and Beavo, 1985; Gillespie and Beavo, 1988; Orlov, Kalinin, Orlova, and Freidin, 1988) and electrophysiological (Hestrin and Korenbrot, 1990) studies indicate that the elements in the light-activated pathway that hydrolyzes cGMP are quantitatively similar in their function in rods and cones and unlikely to account for the functional differences. On the other hand, indirect electrophysiological data suggest that the rate of light-dependent changes in Ca concentration are faster in cones than in rods (Nakatani and Yau, 1989; Hestrin and Korenbrot, 1990; Perry and McNaughton, 1991), posing the possibility that a significant functional difference between rods and cones resides in the Ca-dependent modulation of the enzymes of visual transduction. Investigation of the Ca dependence of the enzymes of the cGMP metabolic cycle in cones thus might be of particular value in understanding the functional differences between receptor types. In electrophysiological studies of single cones isolated from a fish retina we have discovered a previously unreported voltage-dependent activation in darkness of the cGMP-gated current. Rispoli and Detwiler (1991) have recently reported a similar current in the transmuted "rods" of Gecko. Here we analyze the mechanism that underlies this current and find that it reflects activation by Ca, in darkness, of the molecular machinery of transduction. Through this analysis we show that in intact cone outer segments, cytoplasmic Ca concentration can be calculated from the kinetic balance between its influx and efflux and that cytoplasmic Ca regulates guanylate cyclase with features indistinguishable from those in rods.

METHODS

Materials

Striped bass (*Morone saxatilis*), obtained from a fish hatchery (Professional Aquaculture Services, Chico, CA), were maintained in the laboratory for up to 4 wk under 12-h dark–light cycles with free access to fish chow. Fish used for experimentation were 7–18 mo old and ranged in body length from 5 to 30 cm. Wheat germ agglutinin (WGA) was received from E-Y Laboratories,

Inc. (San Mateo, CA), BAPTA from Molecular Probes, Inc. (Eugene, OR), MEM vitamins and amino acid supplements from the tissue culture facility at UCSF, and all other chemicals from Sigma Chemical Co. (St. Louis, MO). Purified collagenase (CLSS, 130 U/mg) was purchased from Worthington Biochemical Corp. (Freehold, NJ) and purified DNAaseI (type IV) and hyaluronidase (type 1-S, 290 U/mg) were from Sigma Chemical Co.

Retinal Dissociation and Cell Plating

Fish were dark adapted for 90–120 min and, in complete darkness, were then anesthetized by cold, decapitated, and pithed. Under infrared illumination, aided by a TV camera and monitor, an eye was enucleated and hemisected and the retina was isolated in a standard culture solution of composition (mM): 136 NaCl, 2.4 KCl, 5 NaHCO₃, 1 NaH₂PO₄, 1 MgCl₂, 1 CaCl₂, 10 glucose, MEM vitamins and amino acid supplements, and 10 HEPES, pH 7.5, osmotic pressure 309 mosM. Composition and osmotic pressure of the standard solution were based on measurements of the electrolyte content and osmotic pressure of bass plasma. The isolated retina was incubated for 30–60 s in standard solution supplemented with collagenase, hyaluronidase, and DNAase, each at a concentration of 0.4 mg/ml. After incubation, the retina was washed by transferring it successively through three 10-ml rinses of standard solution in which glucose was isosmotically replaced by 5 mM Na-pyruvate. Finally, the retina was mechanically shredded with fine forceps in 500 µl of the pyruvate-standard solution. 250 µl of the resulting cell suspension, free of retinal fragments, was transferred onto a WGA-coated glass coverslip produced with 1 mg/ml lectin as described by Cherr and Cross (1987). The coverslip formed the floor of a chamber designed for electrophysiological studies. After allowing cells to settle for 15–20 min, the solution in the recording chamber was exchanged for standard, glucose-containing culture solution that included BSA (0.1 mg/ml).

Electrical Recordings

The recording chamber was held on the stage of an inverted microscope equipped with DIC optics. Cells were observed under infrared illumination (860–920 nm) with the aid of a TV camera and monitor. The chamber volume was ~0.5 ml and it was intermittently perfused with the standard incubating solution at a rate of 1–2 ml/min. Membrane currents were recorded from solitary single cones simultaneously with extracellular suction electrodes (Baylor, Lamb, and Yau, 1979) and tight-seal electrodes in the whole-cell configuration (Hamill, Marty, Neher, Sackmann, and Sigworth, 1981). The suction electrode engulfed the cone outer segment, while the tight-seal electrode was applied onto the inner segment. Suction electrodes were fabricated from 7052 glass (Corning Inc.; borosilicate, 1.5/1.1 mm o.d./i.d.) with typical tip opening of 6–6.5 µm (tip resistance 0.9–1.5 MΩ). Tight-seal electrodes were fabricated from Corning 1724 glass (aluminosilicate, 1.5/1.0 mm o.d./i.d.) with typical tip opening of 0.8–1 µm (tip resistance 3–5 MΩ). Tight-seal electrodes were filled with a solution of the following composition (mM): 105 K-gluconate, 20 K-aspartate, 10 KCl, 10 NaCl, 4 MgCl₂, 3 ATPNa₂, 1 GTPNa₃, and 10 MOPS, 303 mosM osmotic pressure. Solutions of pH 6.75 or 7.25 were used with identical results. In some experiments, the pipette-filling solution also included 5 mM BAPTA (at pH 7.25) titrated with CaCl₂ to obtain a final free Ca concentration of 270 nM. Titration was carried out using a Ca-sensitive electrode constructed as described (Miller and Korenbrot, 1987).

In the course of an experiment, we drew the outer segment of a single cone into a suction electrode and lifted the cell off the coverslip in the recording chamber. We measured photocurrents and, if the cell was healthy, we then formed a giga-seal with the tight-seal electrode on the inner segment and established whole-cell mode with a brief (0.1 ms) voltage pulse. All experiments were carried out at room temperature (21–23°C). A reference electrode

was connected to the recording chamber via a 2% agar bridge containing the standard bath solution. Membrane currents in the suction electrode were measured with a current amplifier (model 8900; Dagan Corp., Minneapolis, MN) and in the tight-seal electrode with a patch-clamp amplifier (Axopatch 1-D; Axon Instruments, Inc., Foster City, CA). Because the currents of interest were both slow and small, capacitance and resistance compensation were not applied. Analogue data were filtered with an 8-pole Bessel filter (902 LPF; Frequency Devices Inc., Haverhill, MA) at 100 Hz for the suction electrode and 300 Hz for the tight-seal electrode. Data were digitized on-line at 625 Hz with 12-bit accuracy and stored for later analysis (Fastlab System; Indec Systems, Inc., Sunnyvale, CA). The suction electrode currents, which lack an absolute reference, were defined to be zero at the holding voltage in the dark. Positive values for these currents correspond to photocurrents as conventionally defined. In the tight-seal electrode data, as is usual, inward currents were defined as negative and membrane voltage was defined with the extracellular space as ground. Numerical solutions of differential equations and simulations were carried out using Tutsim (Applied i, Palo Alto, CA) and curve fitting was executed with a nonlinear, least-squares minimization algorithm (NFIT; Island products, Galveston, TX).

Photostimulation

Stimuli of unpolarized light were presented to the entire photoreceptor through the objective of the microscope used for viewing the cells. Using a narrow band interference filter (± 10 nm half-bandwidth) 540-nm light was selected to be delivered either continuously or as 10-ms duration flashes. Light intensity was controlled with neutral density filters and measured with a calibrated photodiode placed at the position of the photoreceptors on the microscope stage.

RESULTS

Mechanical dissociation of the retina of striped bass yielded solitary single and twin cone photoreceptors that were anatomically incomplete: they included the outer segment and portions of the inner segment (the ellipsoid and myoid) but lacked the nuclear region and synaptic pedicle. Solitary cones, both single and twin, remained viable in culture for up to 4 h and generated photoresponses that were indistinguishable from those measured in intact, isolated retinas. All experiments reported here were carried out with solitary single cones.

Dark, Voltage-activated Current in the Cone Outer Segment

We used suction electrodes to specifically measure the current of the outer segment membrane. Simultaneous use of tight-seal electrodes in the whole-cell mode allowed us to control membrane voltage. Fig. 1 illustrates membrane currents generated by changes in voltage in a single cone studied simultaneously with suction and tight-seal electrodes. Membrane voltage was held at -40 mV and was then stepped to values in the range between -90 and $+60$ mV. Panels on the left illustrate data collected with the suction electrode, while those on the right illustrate currents measured with the tight-seal electrode. In each panel, the currents illustrated on top were measured in darkness, whereas those on the bottom were measured in the presence of continuous illumination. The data shown are typical of every cell studied with this protocol ($n = 30$). At -40 mV holding potential in the dark, the net membrane current measured with the tight-seal electrodes was nearly zero. This near-zero sum arises from the balance between two coexisting dark current loops: one that flows inward

into the outer segment and one the flows outward from the inner segment (for reviews see Baylor, 1987; McNaughton, 1990).

By convention, the outer segment current measured with the suction electrode in the dark was defined as zero in amplitude at the holding voltage. In reality, as
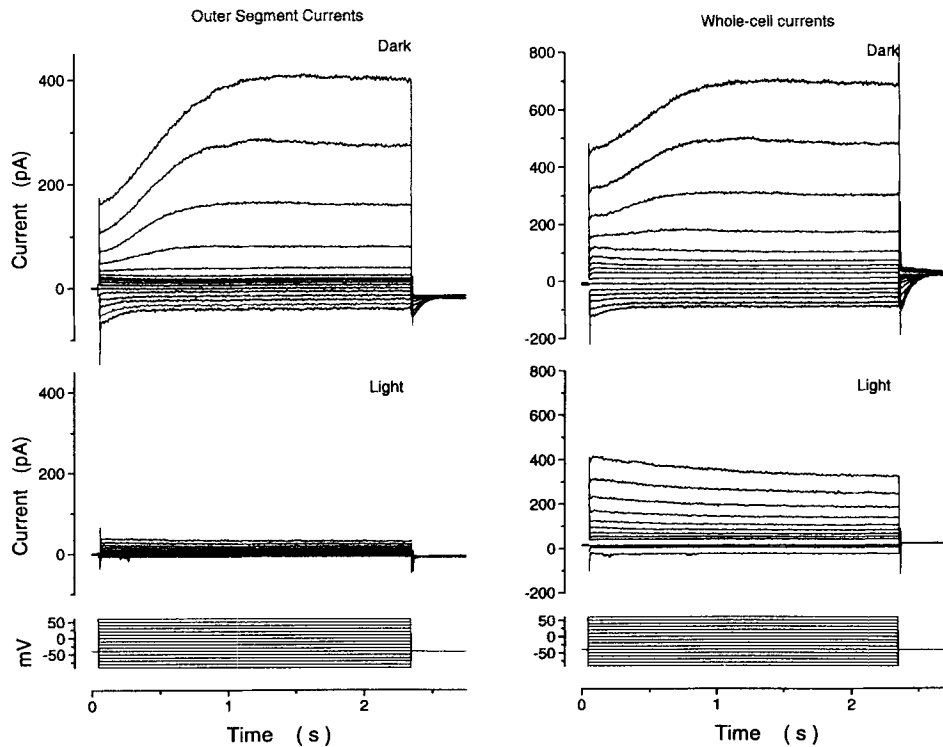

FIGURE 1. Voltage-dependent membrane currents in a single bass cone. Left panels illustrate outer segment currents measured with suction electrodes either in the dark (*top panel*) or under bright, continuous illumination (540 nm light, 7.2 × 10⁶ photons/μm² s) (*bottom panel*). Right panels illustrate whole-cell currents measured simultaneously with a tight-seal electrode either in darkness (*top panel*) or under continuous illumination (*bottom panel*). Capacitative currents were digitally removed from the records. Membrane voltage was held at −40 mV and 2.3-s duration voltage steps were delivered at 5-s intervals. The steps covered the range between −90 and +60 mV in 10-mV intervals. By convention, suction electrode currents were defined as zero amplitude at the holding voltage in the dark. Tight-seal electrode current amplitudes were measured in absolute units and positive values were assigned to outward currents. Outer segment currents in the dark were voltage and time dependent: voltages more depolarizing than +10 mV activated outward currents with a sigmoidal time course that was entirely suppressed by light. We call these currents DVAC.

pointed out above, the outer segment sustained an inward current at the holding voltage. Hyperpolarization enhanced the inward current in the outer segment and at voltages more hyperpolarized than −60 mV the current inactivated slowly. Depolarization generated positive currents in the outer segment that were time independent

for voltages up to 0 mV, but exhibited a pronounced time-dependent activation at voltages above +10 mV (Fig. 1). The outward outer segment currents observed at voltages above +10 mV increased in amplitude with an approximate sigmoidal time course up to a steady state. We call this dark, voltage-activated current (DVAC). DVAC in the outer segment was entirely suppressed by light. The membrane resistance in the light was voltage independent and had a value, on average, of 2.9 × 10^9 Ω (Fig. 1). The complete suppression of DVAC by light and the high value of membrane resistance in the light suggests that the plasma membrane in the outer segment of cones contains only one class of ion channels, those sensitive to light, and that DVAC arises from their specific activation.

Tight-seal electrode recordings in the dark also showed DVAC as an outward current with a sigmoidal time course at voltages higher than +10 mV. Under illumination DVAC disappeared, but light-insensitive currents of appreciable amplitude were still apparent (Fig. 1). Light-insensitive currents arise from the activity of various time- and voltage-dependent ion channels located in the cone inner segment membrane (Maricq and Korenbrot, 1988, 1990*a*, *b*; Barnes and Hille, 1989). The time course and amplitude of DVAC, measured in the tight-seal electrode recordings as the difference between currents measured in the dark and those measured in light, were essentially identical to those measured with the suction electrode in the same cell.

Electrical Properties of DVAC

To test the thesis that DVAC arises from activation in darkness of the light-sensitive, cGMP-gated channels in the cone outer segment membrane, and not from activation of a different class of ion channels, we analyzed and compared the current–voltage (*I-V*) characteristics of the photocurrent with those of DVAC. To determine the *I-V* curve of the photocurrent, we measured the difference in current amplitude between a time point immediately preceding presentation of a saturating flash of light and a point at the peak of the photocurrent (Fig. 2). We repeated this measurement at each voltage tested in both suction and tight-seal electrode recordings. To determine the *I-V* curve of DVAC in both suction and tight-seal electrode data, we measured, at each voltage, the difference in current amplitude at the same time point before and after continuous illumination (Figs. 1 and 2). *I-V* curves of DVAC were measured at both early and late time points. Early time points were measured 60–90 ms after the onset of the voltage pulse, just at the end of the capacitative current. Late time points were measured when the activated currents had just reached their steady-state value. These time points ranged between 0.75 and 1.5 s for all cells studied (*n* = 9). The form of the *I-V* curve of the light-sensitive current in single cones of bass is similar to that previously reported for other single cones (Attwell, Werblin, and Wilson, 1982) and is well described by the empirical function (Fig. 2):

$$I(v) = A_1 \exp\left[(1 - \gamma)\left(\frac{V - V_r}{V_o}\right)\right] + A_2 \exp\left[(-\gamma)\left(\frac{V - V_r}{V_o}\right)\right] \qquad (1)$$

where A_1 and A_2 are current amplitudes and γ, V_r, and V_o are adjustable parameters. The same function, with different values for the adjustable parameters, describes the *I-V* of the photocurrent in other photoreceptors (for review see Yau and Baylor,
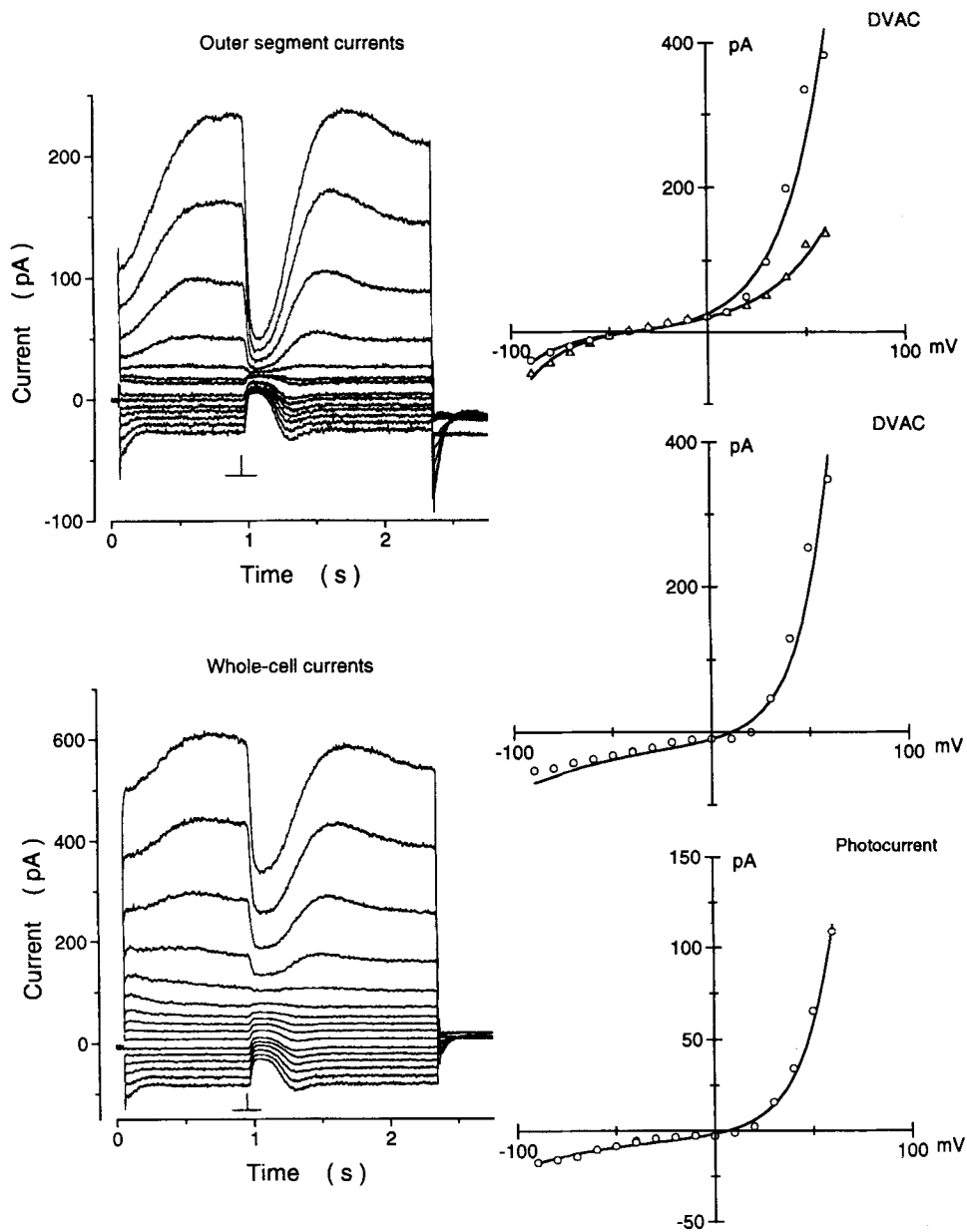
FIGURE 2. Voltage- and light-dependent membrane currents in a single cone. The panels on the left illustrate currents measured simultaneously with a suction electrode (*top panel*) and a tight-seal electrode (*bottom panel*) in response to voltage steps. Capacitative currents were digitally removed from the records. In darkness, voltage was held at −40 mV and 2.3-s duration voltage steps were delivered at 15-s intervals. The steps covered the range between −90 and +60 mV in 10-mV intervals. At the time indicated by the vertical dash a 10-ms duration flash sufficient to saturate the photocurrent amplitude was delivered (540 nm, 5.8 × 10³ photons/μm²). The *I-V* curves of DVAC in the right panels were measured from the

1989). Nonlinear, least-squares fits of the equation to data for 10 cells had the following average values ($\pm$SD): γ = 0.20 ($\pm$0.01), V_r = -10.12 ($\pm$0.67), and V_0 = 12.51 ($\pm$0.09).

The *I-V* curves of DVAC, measured either in the suction or the tight-seal electrode recordings, were also fit very well by Eq. 1 (Fig. 2). The fit to the early DVAC *I-V* curves measured in nine different cells had the following average values ($\pm$SD): γ = 0.46 ($\pm$0.11), V_r = -10.73 mV ($\pm$1.15), and V_0 = 12.55 ($\pm$0.82). The fit to the late DVAC *I-V* curves measured in the same cells had the following average values ($\pm$ SD): γ = 0.38 ($\pm$0.10), V_r = -10.56 ($\pm$1.66), and V_0 = 12.36 ($\pm$0.42). Thus, the quantitative description of the shape of the *I-V* curves of light-sensitive and DVAC currents is the same. An even more significant similarity lies in the fact that the reversal potential of the light-sensitive current was 13.4 mV ($\pm$2.6) (n = 14), while that for DVAC (measured only from the tight-seal electrode data) was 12.5 ($\pm$4.3) (n = 5). Thus, DVAC and the photocurrent arise from the activity of ion channels of essentially identical conductance and reversal potential.

To further test the thesis that DVAC is generated by additional activation of the outer segment channels normally opened in darkness, we analyzed tail currents associated with DVAC. If DVAC arises from activation of one class of channels with a single reversal potential, then the development of the instantaneous amplitude of tail currents that appear in counterpart with DVAC should faithfully match the time course of DVAC; failure of this expectation would suggest that currents with more than one reversal potential contribute to DVAC. To apply this test we measured outer segment currents in response to repeated voltage steps to $+50$ mV that were progressively longer in duration (Fig. 3). The outward currents activated by depolarization superimposed fully in repeated trials. The return of the voltage to its holding value generated instantaneous inward tail currents that decayed with the time course of a single exponential. We determined the instantaneous amplitude of the tail currents by fitting a first-order exponential to the decaying current and extrapolating it to the instant of the voltage change. In Fig. 3 the instantaneous amplitude is indicated by open circles at the beginning of each tail current. This figure illustrates that, indeed, the time course of development of the instantaneous tail current amplitude was identical to that of DVAC, represented by the continuous line that joins the open circles. This finding, again, confirms that DVAC arises from additional

---

data shown in Fig. 1, whereas that of the photocurrent was measured from the data in Fig. 2. The uppermost *I-V* curve is that of DVAC as measured from the suction electrode data. Current amplitude was measured 90 ms after the onset of the voltage step (early DVAC, *triangles*) or in the steady state, 1.2 s after voltage onset (late DVAC, *circles*). By convention the current measured with the suction electrode was defined to be of zero amplitude at the holding voltage. We determined the absolute position of the *I-V* curve of DVAC (*middle panel*) from the tight-seal electrode data by measuring, at each voltage, the difference in amplitude in the currents measured in the dark and under continuous illumination. The bottom panel is the *I-V* of the photocurrent. This curve is the same for suction and tight-seal electrode data (*open circles*) and was calculated by measuring, for each voltage, the peak amplitude of the current change caused by the stimulus flash. The continuous line in each of the *I-V* panels is an optimized fit to the data of an equation (Eq. 1).

activation, by voltage and in the dark, of the cGMP-gated channels of the cone outer segment.

Voltage Dependence of DVAC Activation

To analyze in detail the voltage dependence of DVAC activation we measured, for voltages between −90 and +60 mV, the difference between the initial amplitude of the outer segment current (measured 60–90 ms after the onset of the voltage) and the steady-state amplitude (Fig. 1). Since the currents were measured at constant voltage, the increase in current amplitude measures the enhancement in membrane conductance underlying DVAC. To compare data among different cells, we normalized the conductance enhancement at each voltage by dividing it by the enhancement at +60 mV. For voltages between −40 and 0 mV, there was no enhancement of
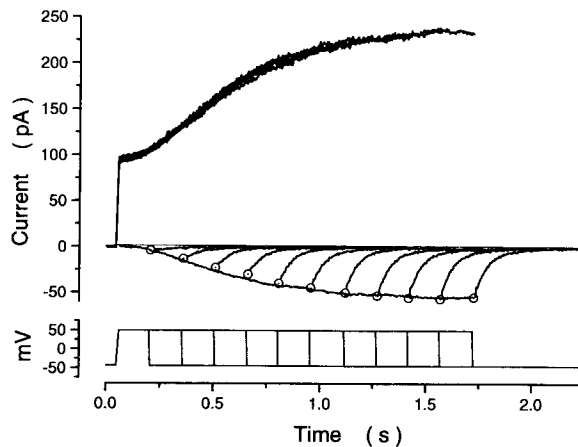

FIGURE 3. Comparison between the time course of development of DVAC and that of the instantaneous tail current amplitudes. Illustrated are outer segment currents measured in a single cone with a suction electrode in response to voltage steps of constant amplitude and progressively longer duration. For clarity, capacitative currents have been digitally removed from the records displayed. Membrane voltage was held at −40 mV. Steps in voltage to +50 mV ranging in duration between 150 ms and 1.65 s in 150-ms increments were repeated at 5-s intervals. Instantaneous tail current amplitude for each voltage step is indicated by an open circle. The continuous line that joins the open circles describes the time course of DVAC and it is the same as the positive current measured in response to the longest duration pulse, scaled by −0.4.

conductance (Figs. 1 and 2). Above 0 mV, the conductance increase with voltage was well described by the Boltzmann equation (Fig. 4):

$$\frac{\Delta g(V)}{\Delta g_{max}} = \left[1 + \exp\left(\frac{V - V_o}{k}\right)\right]^{-1} \tag{2}$$

where $\Delta g(V)/\Delta g_{max}$ is the normalized conductance enhancement, V_o is the membrane voltage at the midpoint of activation, and k describes the steepness of the voltage dependence. For 10 cells, the average values of these constants were (±SD) V_o = 28.7 mV (±2.7) and k = 5.6 (±1.2), and the maximum conductance enhancement was 2.79 (±0.64).

Voltage Dependence of the Photocurrent Time Course

Data shown in Fig. 2 demonstrate that membrane voltage not only activates DVAC, but also affects the kinetics of the photoresponse. At the holding potential of -40 mV, the time course of the voltage-clamped photocurrent elicited by a dim flash of light was well described by the function (Fig. 5):

$$I(t) = A_1 \left[\frac{t}{t_{peak1}} * \exp\left(1 - \frac{t}{t_{peak1}}\right) \right]^{n_1-1}$$
$$+ A_2 \left(1 - \exp\frac{t}{\tau}\right)\left[\frac{t}{t_{peak2}} * \exp\left(1 - \frac{t}{t_{peak2}}\right)\right]^{n_2-1} \tag{3}$$

This function is a modification of that used by Baylor, Hodgkin, and Lamb (1974) to describe the kinetics of photovoltages in turtle cones. The function is the sum of two independent impulse responses of a sequence of n first-order reactions. The
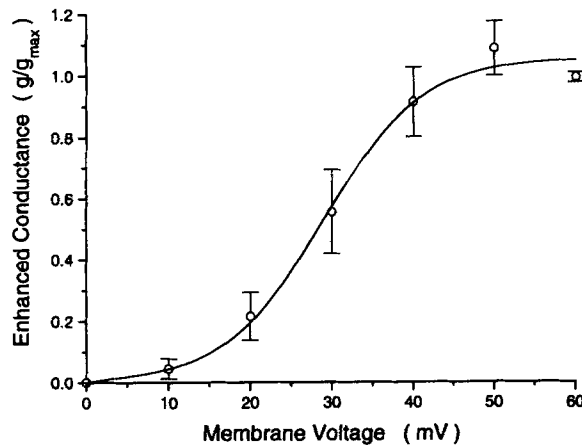

FIGURE 4. Voltage dependence of DVAC. The enhancement in outer segment conductance in darkness at voltages above 0 mV was measured from data such as those in Fig. 1 in 10 different single cones. To compare results among the cells we normalized the data: for each cell, the conductance enhancement at each voltage was divided by the enhancement measured at $+60$ mV. The data points are the average $\pm$ SD. The continuous line is an optimized fit to the data of Boltzmann's equation (Eq. 2).

subscripts 1 and 2 identify the two impulse responses. A_1 and A_2 are the current amplitudes, t_{peak1} and t_{peak2} are the times to the response maxima and minima, and n is the number of reactions in the sequence. The amplitude of the impulse response 2 rises exponentially with time constant τ. The average values of these parameters that best fit the photocurrent measured at the holding potential in response to dim flashes for 10 cells were: $A_1 = 3.32$ pA (± 1.2), $t_{peak1} = 0.086$ s (± 0.012), $n_1 = 3.45$ (± 0.69), $A_2 = 0.80$ pA (± 0.40), $t_{peak2} = 0.19$ s (± 0.05), $n_2 = 7.25$ (± 2.76), and $\tau = 0.244$ s (± 0.08).

To illustrate the effects of membrane voltage on photoresponse kinetics, we compare in Fig. 5 the photocurrents measured in the same cell in response to the identical flashes, either dim or bright, presented after membrane currents had reached steady state, following a step change in membrane voltage. To compare their kinetics, the amplitude and polarity of the photocurrents were arbitrarily scaled to the same peak value. Hyperpolarizing voltages up to -90 mV did not change

photoresponse kinetics at all when compared with those measured at the holding voltage, and Eq. 3 fit the data very well. Depolarizing voltages above +10 mV and up to +60 mV modified the response kinetics in the same qualitative manner: the initial rate of response was slightly slowed down, with an average decrease in the initial slope of ~10–15% at the largest depolarizations. The recovery of the current from its
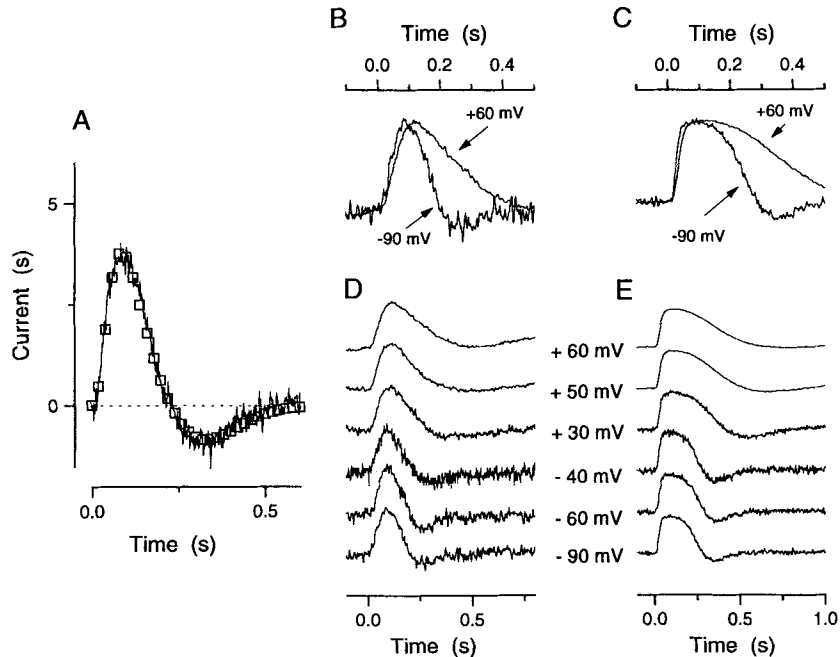

FIGURE 5. Voltage dependence of the photocurrent. Photocurrents shown were measured with a suction electrode. A illustrates the photocurrent measured at −40 mV holding potential and generated in response to a 10-ms duration flash of 540-nm light delivering 80 photons/ μm^2. Superimposed on the data is the best fit of the function given in Eq. 3. D and E illustrate the photocurrent generated in the same cone by dim flashes (panel D, 80 photons/μm^2) or bright flashes (panel E, 5,800 photons/μm^2) delivered in the steady state at each of the membrane voltages indicated. The amplitude and polarity of these signals were arbitrarily scaled to display the same peak amplitude. Unscaled data for a different cone are shown in Fig. 2. B and C display superimposed, scaled photocurrents measured in response to dim (B) or bright (C) flashes delivered in the steady state at −90 or +60 mV, as indicated. The data at −90 mV were identical to those measured at all voltages between −90 and 0 mV. For positive membrane voltages, the photocurrent kinetics were slowed down, slightly at the onset of the response and markedly at its offset.

peak to its initial value, on the other hand, was substantially slowed down as the depolarizing voltage increased in amplitude. In the example shown, the slowdown of the recovery phase of the photoresponse was sufficient to eliminate the typical undershoot observed at holding potential. The results shown are typical of every cell studied with this protocol ($n = 8$).

A Mechanism to Explain DVAC: The Effects of Cytoplasmic BAPTA

The gating activity of cGMP-gated channels in cones is voltage independent (Haynes and Yau, 1990). Therefore, DVAC must arise from a voltage-dependent process that controls the concentration of cGMP in the dark, but not from control of the channels themselves. A simple possible mechanism to explain DVAC, based on the known biochemical events of phototransduction in rods, could be as follows: First, membrane depolarization reduces Ca influx into the outer segment because of a decrease in its electromotive driving force. Second, a reduced influx of Ca, in the presence of continuous efflux via the Na/Ca,K exchanger, causes a decrease in cytoplasmic Ca concentration in the outer segment. Third, this reduction in Ca activates guanylate cyclase causing, fourth, synthesis of cGMP and an increase in its cytoplasmic concentration. Since PDE is active to a limited extent even in darkness (Goldberg, Ames, Gander, and Walseth, 1983; Hestrin and Korenbrot, 1987; Sather and Detwiler, 1987; Hodgkin and Nunn, 1988), the enhanced cGMP concentration increases PDE activity (substrate level activation) until the activities of the two enzymes, cyclase and PDE, come to a new steady state. The increase in cGMP concentration above its normal level in darkness opens the cGMP-gated channels, leading to an increase in membrane conductance. Under voltage clamp the enhanced conductance causes an increase in current amplitude, as we observe. DVAC is suppressed by light because any voltage-dependent enhancement in cGMP concentration due to guanylate cyclase activation is obliterated by the dominant activity of the light-activated PDE.

The most direct experimental test of this model is to examine the effects of a Ca buffer, loaded into the cytoplasm of the cones, on the features of DVAC. If changes in membrane voltage are linked to activation of cGMP-gated channels by changes in cytoplasmic Ca concentration, then DVAC should become much smaller in amplitude and slower in time course in the presence of cytoplasmic Ca buffer. We loaded BAPTA (5 mM), titrated to yield 270 nM free Ca concentration, into single cones through the tight-seal electrode and examined DVAC in these cells. Upon rupture of the membrane under the electrode the holding current increased, on average, by 9.8 pA ($\pm$5.7, n = 5). That BAPTA was indeed loaded into the outer segment cytoplasm was evident by the changes in photocurrent kinetics: in every cell studied (n = 5), BAPTA slowed down the time course and increased the sensitivity of the photocurrents relative to those measured in control cones not loaded with BAPTA (Fig. 6). These characteristic effects of cytoplasmic Ca buffers on photocurrent kinetics and sensitivity have been extensively analyzed in rods (Korenbrot and Miller, 1986; Torre et al., 1986; Matthews, 1991).

BAPTA, as expected from the model, attenuated the amplitude and slowed down the time course of DVAC without affecting its *I-V* characteristics or reversal potential (Fig. 6). Comparison of data in Figs. 1 and 6 shows that in the presence of BAPTA, membrane depolarization up to +60 mV did not produce the typical large and rapid sigmoidal enhancement of current amplitude. Of eight cells studied, DVAC was entirely blocked in two and strongly attenuated in all others. In control cones, the maximum conductance enhancement was, on average, 279% ($\pm$64% SD), but it was only 37% ($\pm$26% SD) in BAPTA-loaded cones.

In those cells in which DVAC of any amplitude was discernible ($n = 6$), the I-V relationship of DVAC currents at early times was well described by Eq. 1 with average values of the constants ($\pm$SD): $\gamma = 0.47$ (± 0.11), $V_r = -11.07$ (± 2.05), and $V_0 = 12.38$ (± 0.20). I-V curves of DVAC at late times were also well described by Eq. 1 with
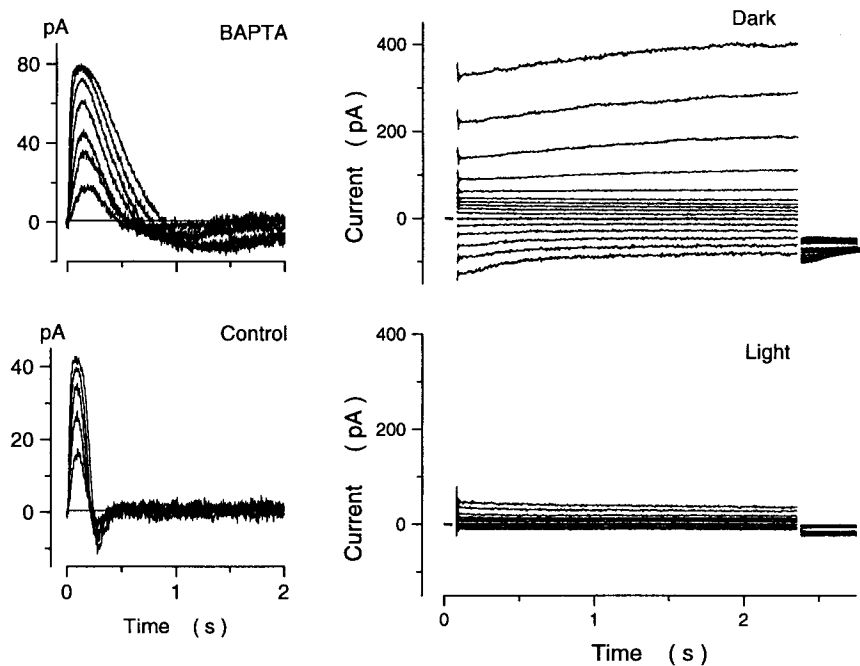

FIGURE 6. Effect of 5 mM cytoplasmic BAPTA on the kinetics of cone photocurrents and DVAC. Photocurrents in the top left panel were measured with a suction electrode under voltage clamp at -40 mV holding potential in a cone loaded with 5 mM BAPTA. Shown are currents generated by 10-ms duration flashes of 540-nm light presented at 15-s intervals. Flash intensities tested were (in photons/μm^2): 54, 157, 322, 683, 1,568, 2,981, and 5,839. The bottom left panel illustrates photocurrents measured under the same conditions in a control cone; that is, one not loaded with BAPTA. Shown are photocurrents generated by 540-nm flashes of the following intensities (in photons/μm^2): 157, 322, 683, 1,568, and 2,981. The right panels illustrate outer segment currents measured with suction electrodes either in the dark (*top*) or under bright, continuous illumination (540 nm light, 7.2×10^6 photons/μm^2 s) (*bottom*) in the BAPTA-loaded cone whose photoresponses are shown in the top left panel. Capacitative currents were digitally removed from the records. Membrane voltage was held at -40 mV and 2.3-s duration voltage steps were delivered at 5-s intervals. The steps covered the range between -90 and $+60$ mV in 10-mV intervals. The light-sensitive currents failed to demonstrate the typical time-dependent enhancement (DVAC) characteristic of control cells.

average values ($\pm$SD): $\gamma = 0.47$ (± 0.11), $V_r = -10.45$ (± 0.78), and $V_0 = 12.22$ (± 0.70). The reversal potential of DVAC in these cells (measured in the tight-seal electrode data only) was $E_{rev} = 13.1 \pm 4.3$ mV ($n = 5$). In only three cells was DVAC of sufficient amplitude to reliably investigate the voltage dependence of its activation.

In these cells, the voltage dependence was well described by Boltzmann's equation (Eq. 2), with V_0 = 23.0 mV ($\pm$2.69) and k = 4.37 ($\pm$0.59). Thus, Ca buffering did not alter the intrinsic properties of the cGMP-gated channels, but severely attenuated their time-dependent activation by voltage in darkness.

THEORY

To further test the adequacy of the model to explain DVAC, we simulated the time course and voltage dependence of outer segment conductance by mathematically modeling each step described above. In the following section we define and justify the quantitative features assigned to each step in the model under the simplest possible assumptions.

Voltage Dependent Decrease in Cytoplasmic Ca Concentration

Ca ions permeate through the light-sensitive, cGMP-gated channels of the cone outer segment (Perry and McNaughton, 1991). We assume that, as in rods, in the dark and at the holding potential of -40 mV, there is a sustained inward Ca flux through these channels that is balanced by an equal Ca efflux through a Na/Ca,K exchanger (Yau and Nakatani, 1985; Miller and Korenbrot, 1987). The net Ca flux in darkness is zero. A depolarizing step change in membrane voltage reduces Ca influx because its electromotive force is reduced as the equilibrium potential of Ca is approached. The voltage-dependent decrease in Ca influx, in the face of sustained Ca efflux via the Na/Ca,K exchanger, leads to lowering of cytoplasmic Ca concentration (Yau and Nakatani, 1985). While holding at command voltages ≥ 10 mV, however, the decrease in Ca influx upon depolarization is followed by an increase that reflects the activation of membrane conductance underlying DVAC. That is, at voltages > 10 mV, cytoplasmic Ca concentration should initially decrease and then partially recover as Ca reenters the outer segment through the enhanced conductance.

We calculated for each cell the time course of the change in cytoplasmic Ca concentration caused by voltage with the method detailed in the Appendix. The method of calculation is similar to that previously used to successfully model light-dependent changes in Ca concentration measured in the extracellular space of rod outer segments (Miller and Korenbrot, 1987). The method of calculation describes the change in Ca concentration from an assigned starting value of 270 nM in the dark at -40 mV. This assignment was based on direct measurements of cytoplasmic free Ca in dark-adapted rod outer segments (Ratto et al., 1988; Korenbrot and Miller, 1989). This is a reasonable value for single cones as well, since recordings with tight-seal electrodes filled with BAPTA-buffered solutions containing 270 nM free calcium changed the outer segment dark current by only ~ 10 pA on average (see Results).

It is critical to note that the simulation of changes in cytoplasmic Ca concentration depends on two adjustable parameters: (a) the voltage dependence of the Ca flux through the cGMP-gated conductance, a property that has not been investigated directly, and (b) the time constant of Ca efflux from the outer segment via the Na/Ca,K exchanger, τ_{ex}. In simulations we imposed the constraint that the starting value of τ_{ex} was 130 ms at $+50$ mV. We imposed this constraint because in rods τ_{ex}

can be approximately measured from the exponential decline of the electrogenic activity of the exchanger transport observed when all outer segment channels are suddenly closed by light (Yau and Nakatani, 1985). This electrogenic activity is also observed in cones under voltage clamp (Hestrin and Korenbrot, 1990; Perry and McNaughton, 1991), including those of bass (our unpublished observations). In single bass cone the average value of τ_{ex} at -40 mV was 111 ms (± 11.3, $\pm$SD; $n = 5$).

Ca-dependent Regulation of Guanylate Cyclase

The kinetics of guanylate cyclase and the features of its possible regulation by Ca are unknown in cones. We assumed that the enzyme in cones is functionally the same as that in rods (Koch and Stryer, 1988; Koch, Eckstein, and Stryer, 1990). Based on the experimental findings in rods we assumed the velocity of guanylate cyclase (V_{GC}) to consist of a basal, Ca-independent activity of 4 μM/s (V^*_{GC}) and a Ca-dependent activity ($V_{GC}([Ca]_i)$.

$$V_{GC} = V^*_{GC} + V_{GC} ([Ca]_i) \tag{4}$$

The Ca-dependent activity is given by Koch and Stryer (1988):

$$V_{GC} ([Ca]_i) = V^{max}_{GC} * \frac{[GTP]}{K_m + [GTP]} * \frac{\left(\dfrac{1}{[Ca]_i(V, t)}\right)^n}{\left(\dfrac{1}{K_d}\right)^n + \left(\dfrac{1}{[Ca]_i(V, t)}\right)^n} \tag{5}$$

where V^{max}_{GC} is the enzyme's maximum velocity, which has a value of 95 μM/s (Koch and Stryer, 1988; Koch et al., 1990). K_m is the Michaelis constant of the enzyme for GTP. The value of K_m was taken to be 1 mM, as reported for the enzyme in rods (Krishnan, Fleischer, Chader, and Krishna, 1978; Fleischman and Denisevich, 1979; Koch et al., 1990). Guanylate cyclase activity depends only on cytoplasmic Ca concentration because the concentration of GTP can be expected to remain constant at 1 mM since this is the concentration of the nucleotide in the solution that fills the tight-seal electrode, which acts as an infinite source of GTP. The cytoplasmic Ca concentration is $[Ca]_i(V,t)$. K_d is the Ca binding constant of the enzyme and n is a cooperativity factor. From data in rods we assigned $n = 4$ and $K_d = 90$ nM (Koch and Stryer, 1988).

Time-dependent Increase in Cytoplasmic cGMP Concentration

cGMP concentration must rise as guanylate cyclase activity increases in the dark. In intact photoreceptors, even in darkness, the PDE is active (Goldberg et al., 1983; Hestrin and Korenbrot, 1987; Sather and Detwiler, 1987; Hodgkin and Nunn, 1988). Therefore, to calculate the change in cGMP concentration it must be considered that an increase in cGMP synthesis after activation of guanylate cyclase is opposed by PDE activity. PDE activity is stimulated by the rise in cGMP concentration itself (substrate level activation). The time course of the change in cGMP concentration is the solution of the following differential equation:

$$\frac{d[cGMP](t)}{dt} = V_{GC} - k^d_{PDE} * [cGMP](t) \tag{6}$$

where V_{GC} is given by Eqs. 4 and 5. k^d_{PDE} is the pseudo first-order rate constant of PDE in the dark and $[cGMP](t)$ is the cytoplasmic concentration of cGMP. This equation considers that PDE activity is of first order because the cytoplasmic concentration of cGMP in darkness, ~ 12.8 μM (see below for justification), is well below the range of values reported for the K_m for cGMP of PDE in rods and cones (review in Pugh and Cobbs, 1986; Gillespie and Beavo, 1988; Orlov et al., 1988).

Activation of Membrane Conductance by cGMP

Studies on membrane patches detached from bass single cone outer segments (Picones and Korenbrot, 1992) indicate that membrane conductance increases with cGMP concentration with a dependence well described by:

$$\frac{g(t)}{g_{max}} = \frac{([cGMP](t))^{2.5}}{(K_{cGMP})^{2.5} + ([cGMP](t))^{2.5}} \tag{7}$$

where $g(t)$ is membrane conductance, g_{max} is the maximum value of this conductance, $[cGMP](t)$ is the cytoplasmic concentration of cGMP (Eq. 6), and K_{cGMP} is the binding constant of the ion channel for cGMP. The value of K_{cGMP} in bass cones is 42 μM (Picones and Korenbrot, 1992). A similar value for K_{cGMP} was first reported for cones of the catfish retina (Haynes and Yau, 1985).

Eq. 6 can be used to define the concentration of cGMP in the dark. In cones, as in rods, only a small fraction of the available cGMP-gated channels are normally open in the dark: the dark current amplitude is only 3–10% of the maximum current amplitude elicited by saturating levels of cytoplasmic cGMP (Cobbs, Barkdoll, and Pugh, 1985). In our simulations, therefore, we assigned $g(t)/g_{max}$ a value of 5% in darkness. Because $K_{cGMP} = 42$ μM in bass cones, this assignment implies that the concentration of cGMP in the dark is 12.8 μM.

Fit of Experimental Data with Simulations

We compared experimental data with the results of simulations obtained by solving the system of equations defined above. To start the simulations, we defined initial conditions in the dark at -40 mV. Given a Ca concentration of 270 nM, Eq. 5 indicates that the guanylate cyclase activity should be 4.58 μM/s. To be in steady state, therefore, PDE activity must also be 4.58 μM/s. Since the concentration of cGMP is 12.8 μM, the first-order rate constant of PDE, k_{PDE}, should be 0.357 s^{-1}.

In simulation three parameters were adjusted: the voltage dependence of Ca conductance through the outer segment channels, the time constant of transport through the Na/Ca,K exchanger, and the buffering power of the cytoplasm for Ca. These parameters determined the magnitude and time course of voltage-dependent changes in cytoplasmic Ca (Appendix). Simulated changes in cytoplasmic Ca concentration were then used to calculate the outer segment membrane conductance using the equations described above.

Calculations with this model simulated experimental data well (Fig. 7). Optimum matches of similar quality (squared difference between experimental and simulated data $\leq 5 \times 10^{-4}$) between simulated and experimental data for eight different cells yielded the average values of the adjustable parameters listed in Table I. The
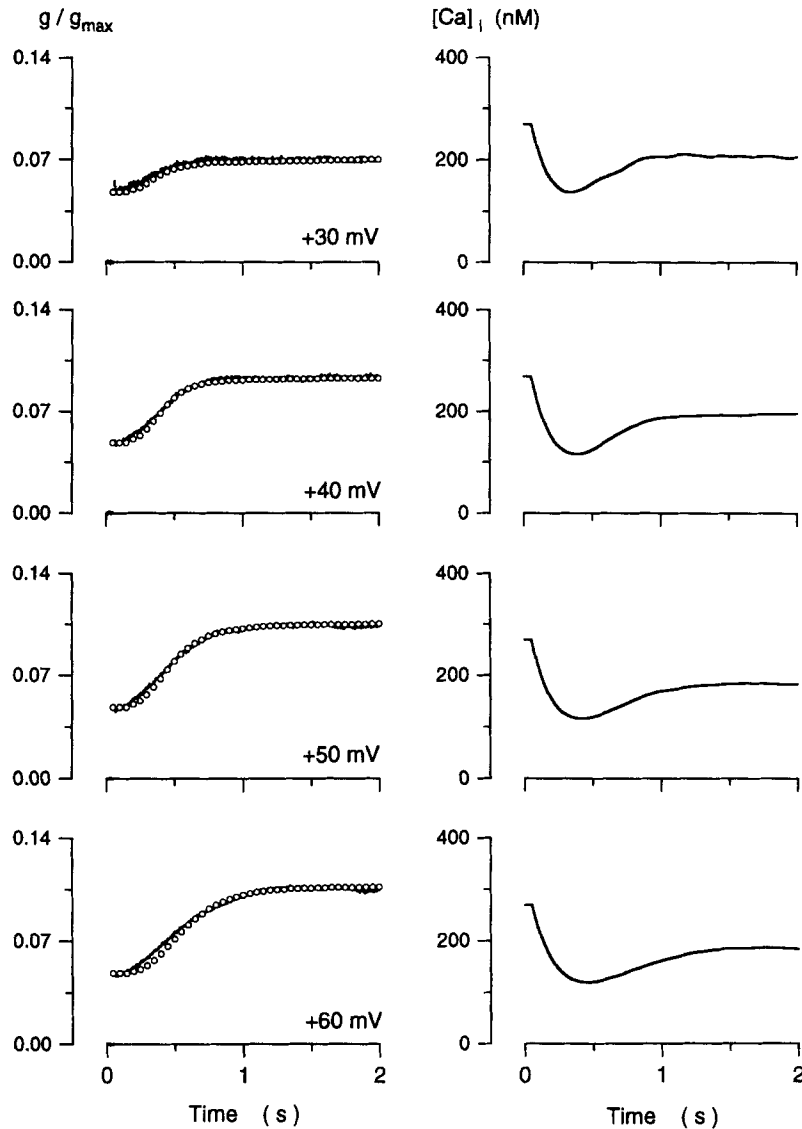
g / g_max

[Ca]_i (nM)

FIGURE 7. Fit to experimental results of data simulated by the model of DVAC detailed in the text. Panels on the left illustrate as a continuous line, cone outer segment membrane conductance measured in the dark in response to depolarizing steps from a holding voltage of −40 mV to +30, +40, +50, or +60 mV, as labeled. The open circles in the left panels represent the outer segment conductance simulated by the model of DVAC. The panels on the right illustrate the simulated changes in cytoplasmic Ca concentration that underlie DVAC. Ca concentration dips to a minimum and then recovers with a nearly exponential time course to a final steady value; both the amplitude of the steady state and the time course of recovery are proportional to membrane voltage. The average values of the adjustable parameters used to obtain fits such as those shown are presented in Table I. The fits shown are typical of our data (squared difference between simulated and experimental data $\leq 4.4 \times 10^{-4}$).

steady-state cytoplasmic Ca concentration was proportional to membrane voltage and, as expected, was progressively lower as the voltage depolarized. Consistent with the saturation of DVAC's conductance enhancement at +50 to +60 mV (Fig. 4), the steady-state cytoplasmic Ca concentrations at these voltages had similar values. The values of τ_{ex} that successfully fit data were close to those expected from direct measurements of this parameter. Moreover, the values of τ_{ex} slowed down as the voltage depolarized, a well-documented feature of the Na/Ca,K transporter (Lagnado and McNaughton, 1990).

To illustrate the kinetic features of the model, Fig. 8 depicts in detail predicted effects of depolarization to +50 mV on the cytoplasmic Ca concentration, the velocity of guanylate cyclase and PDE, the cGMP concentration, and the membrane conductance. The data shown were taken from a successful simulation of experimental results. A critical assumption in the model is that Ca conductance through the cGMP-gated channels is large at voltages $\geq$ +20 mV. This assumption allows the enhanced conductance underlying DVAC to generate a significant time-dependent Ca influx while holding the membrane potential at > +20 mV. The model thus predicts that the cytoplasmic Ca concentration will decrease to a minimum value and

TABLE I

Adjustable Parameters That Best Fit Experimental Data (Mean $\pm$ SD)

V_m	$[Ca]_i$ steady state	$[Ca]_i$ minimum	τ_{ex}	$^Vg_{Ca}/^{-40}g_{Ca}$	Ω	n
mV	nM	nM	ms	γ		
+30	203.6 $\pm$ 8.7	124.6 $\pm$ 14.9	135.6 $\pm$ 24.7	0.85 $\pm$ 0.167	0.04 $\pm$ 0.011	8
+40	183.5 $\pm$ 8.3	109.3 $\pm$ 10.8	147.5 $\pm$ 23.1	0.68 $\pm$ 0.11	0.035 $\pm$ 0.009	8
+50	176.7 $\pm$ 5.5	108.1 $\pm$ 12	159.3 $\pm$ 20.4	0.66 $\pm$ 0.09	0.029 $\pm$ 0.007	8
+60	173.8 $\pm$ 5.3	115.5 $\pm$ 12.4	170 $\pm$ 19.3	0.75 $\pm$ 0.13	0.026 $\pm$ 0.006	8

then recover to a final steady state. Consequently, the guanylate cyclase activity, which tracks the Ca concentration, will also reach a transient maximum value and then be quenched to a steady, less active value. This quenching of activity limits the amount of cGMP produced. The PDE velocity increases in parallel with the rise in cytoplasmic cGMP until it reaches a new value that is in steady state with the activity of guanylate cyclase. When this steady state is reached, the cGMP concentration attains a new, constant value and therefore the membrane conductance also attains a constant value.

DISCUSSION

In single cones isolated from the retina of striped bass, depolarizing membrane voltages activate in the dark an outer segment–specific current we have termed DVAC. DVAC develops with a sigmoidal time course and reflects a voltage-dependent increase in membrane conductance. DVAC is entirely suppressed by light and arises from enhanced activity of the cGMP-gated channels normally controlled by light. This current was not reported in a previous study of the voltage-dependent electrical

properties of cones in the dark carried out with conventional intracellular electrodes (Attwell et al., 1982). DVAC probably was missed because it would have been difficult to separate dark currents specific to the outer segment from all other currents in the isolated cone without the simultaneous use of suction and tight-seal electrodes; in particular, at large depolarizing voltages the inner segment sustains large outward currents through a delayed rectifier K conductance and a Ca-activated Cl conduc-
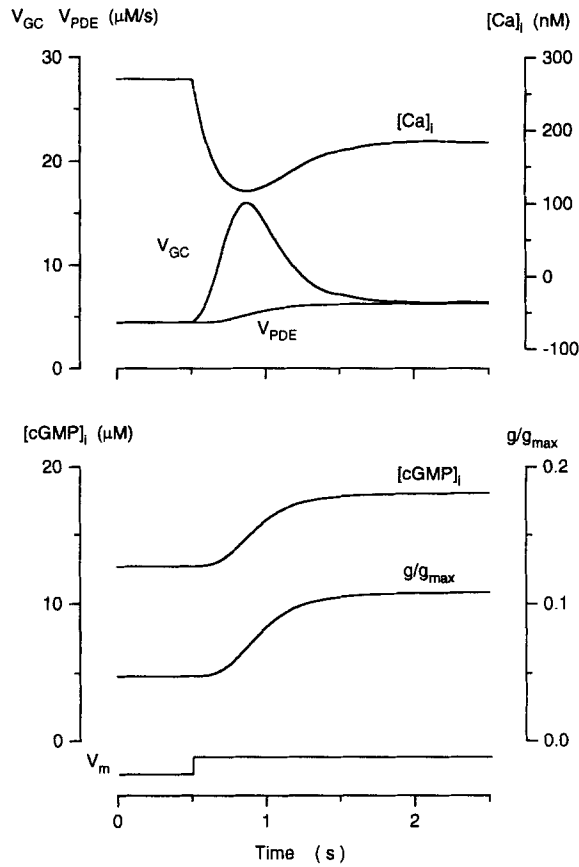

FIGURE 8. Detailed kinetic simulations in the model for DVAC. We illustrate the time course and magnitude of the simulated changes caused by step depolarization from −40 to +50 mV. Data shown successfully fit experimental results. The continuous lines in the top panel are solutions to the system of equations that describe the cytoplasmic concentration of Ca and the velocities of guanylate cyclase (V_{GC}) and PDE (V_{PDE}). The bottom panel illustrates the concentration of cGMP and the normalized membrane conductance (g/g_{max}). The label next to each line identifies the variable illustrated; similar labels on the ordinate identify the units for each variable. At the holding potential (−40 mV), PDE and cyclase velocities are in steady state. Upon depolarization, Ca concentration decreases to a minimum and then recovers to a steady-state value. Cyclase velocity is activated, reaches to a peak, and is then quenched as Ca concentration recovers. PDE velocity rises in parallel with the increase in cytoplasmic cGMP concentration. In the steady state the activities of the two enzymes are again the same and the concentration of cGMP holds at a new, higher value. Membrane conductance increases in parallel with the rise in cytoplasmic cGMP.

tance (Barnes and Hille, 1989; Maricq and Korenbrot, 1990b). Rispoli and Detwiler (1991) have reported the existence in isolated outer segments of Gecko transmuted rods of currents similar in some features to DVAC, but much slower in time course.

The I-V curve of DVAC and its reversal potential are the same as those of the photocurrent. When DVAC is suppressed by continuous illumination, the I-V curve of the outer segment membrane is essentially linear over the range between −90 and

+30 mV with a slope resistance of, on average, 2.9×10^9 Ω. Since the single cone capacitance is, on average, 58.1 pF (SD = ± 13.2, $n = 26$), and assuming 1 $\mu F/cm^2$ for the specific membrane capacitance, then the specific membrane resistance of the outer segment membrane in the light is $\sim 1.6 \times 10^5$ Ω cm^2. In an alternative calculation, assuming disc and plasma membrane are continuous and a disc to disc repeat distance of 300 Å, the surface area of the average single cone outer segment (6 $\mu m \times 15$ μm) is 9.4×10^{-5} cm^2, which yields a specific membrane resistance of 2.7×10^5 Ω cm^2. This large value of specific membrane resistance suggests that the cone outer segment membrane contains very few open channels in the light. That is, the outer segment membrane in cones contains only one class of ion channels, those sensitive to light, and when these close under continuous illumination no other channels are detectable. This conclusion is similar to that previously reached for the outer segment of rod photoreceptors of the tiger salamander, where the slope resistance under continuous illumination is 62×10^9 Ω (Baylor and Nunn, 1986). This calculates to a specific membrane resistance of 4.3×10^5 Ω cm^2, a value similar to that we find for cones.

The cGMP-gated channels in cones are not voltage sensitive (Haynes and Yau, 1990). DVAC, therefore, must be generated not by a direct effect of voltage on channel activity, but indirectly by regulation of cytoplasmic cGMP concentration. We have proposed a specific mechanism to explain DVAC in which depolarizing voltages are linked to changes in cGMP concentration through their effect on Ca flux and cytoplasmic Ca concentration. We envision that depolarizing voltages reduce the dark current carried by Ca through the outer segment channels. Reduced Ca influx, in the presence of continuing efflux via Na/Ca,K exchangers, decreases Ca concentration. The effectiveness of the Ca chelator BAPTA in attenuating DVAC confirms that changes in cytoplasmic Ca link membrane voltage to the activation of the cGMP-gated channels.

We developed a model based on the simplest possible mechanism to quantitatively explain the features of DVAC. The model makes explicit assumptions about the voltage dependence of the Ca flux through the cGMP-gated conductance and thus predicts that depolarization causes a decrease in cytoplasmic Ca that is transient: it first reaches a peak and then recovers to a steady-state value that is lower than that observed at the holding voltage. The transient nature of the Ca concentration change simply reflects the inevitable fact that while holding at depolarized command voltages, the enhanced conductance that underlies DVAC must allow Ca to reenter the outer segment. To successfully simulate experimental data we made explicit adjustments of the Ca conductance of the cGMP-gated channels at the various depolarized voltages tested. Experimental data are not available to compare with the assumed voltage dependence of the Ca conductance.

The decrease in cytoplasmic Ca activates guanylate cyclase. We assumed that the cyclase activity in cones is quantitatively the same as that measured in rods (Fleischman and Denisevich, 1979; Pepe et al., 1986; Koch and Stryer, 1988; Koch et al., 1990). The success of the model indicates that this assumption may be correct and that the cyclase in rods and cones may function with indistinguishable characteristics. Tranchina, Sneyd, and Cadenas (1991) previously reached a similar conclusion in a theoretical model developed to explain properties of adaptation in turtle cones.

The simple mechanism proposed to explain DVAC also invokes an increase in PDE velocity simply because of an increase in concentration of its substrate, cGMP. The linkage between PDE and cyclase activities arises not from unusual coupling mechanisms, but simply from their specific biochemical properties: the K_m of PDE for cGMP makes the activity of the enzyme sensitive to cGMP precisely over the range of concentrations created by the synthetic activity of the cyclase activated by the lowering of Ca concentration. Previous publications, based on both biochemical and electrophysiological experiments, have suggested that the kinetics of light-activated PDE in rods and cones also are essentially the same (Gillespie and Beavo, 1988; Orlov et al., 1988; Hestrin and Korenbrot, 1990). Thus, present evidence suggests that the profound disparities in transduction signal between rods and cones probably arise from differences in the regulation of the activity of the enzymes of transduction, but not from differences in the functional properties of the individual proteins.

A feature of the models is the assumption that in cones PDE is active in darkness. This finding has been demonstrated experimentally in rods (Goldberg et al., 1983; Hestrin and Korenbrot, 1987; Sather and Detwiler, 1987; Hodgkin and Nunn, 1988), but not in cones. Dark PDE activity is of physiological importance. The levels of Ca in the dark in both rods and cones are sufficient to sustain a steady guanylate cyclase activity. Without the balancing activity of PDE, cGMP would continuously accumulate in the dark. PDE activity in the dark also provides a form of cGMP concentration clamp that makes small changes in Ca concentration unable to change cytoplasmic cGMP concentration. This explains why DVAC is apparent only at depolarizing voltages larger than +10 mV: between −40 and +10 mV, Ca concentration does decrease but the magnitude of this change is probably not sufficient to cause net cGMP synthesis.

Rispoli and Detwiler (1991) have reported that detached outer segments of the transmuted rod of Gecko exhibit in darkness a voltage-dependent current that slowly activates with a sigmoidal time course. This current is very similar to DVAC in single cones of fish reported here, but with a time course that is 5–10-fold slower. Baylor and Nunn (1986), in contrast, have reported that in whole rods of tiger salamander the outer segment current in darkness exhibits a voltage-dependent inactivation. The differences in the findings of Rispoli and Detwiler (1991) and Baylor and Nunn (1986) are presently unexplained, but we have found in intact rods of the tiger salamander that the method of whole-cell recording determines the experimental results obtained. Conventional membrane break-through leads to voltage-dependent inactivation similar to the results of Baylor and Nunn (1986); but membrane chemical perforation by Nystatin or Amphotericin B yields results qualitatively similar to those of Rispoli and Detwiler, with a slow and small voltage-dependent activation (Korenbrot, J.I., and J.L. Miller, manuscript in preparation).

The relatively limited extent of the conductance enhancement underlying DVAC and its rapid time course require that the activation of cyclase be transient (see Fig. 8). If cyclase activation were large and sustained, cGMP synthesis would continue, in time resulting in an outer segment current that is larger and slower than what we observed. In the simplest possible model, we have achieved quenching of cyclase velocity by modeling a transient change in cytoplasmic Ca, based on a calculated, but unproven, large Ca conductance through the cGMP-gated channels at depolarizing

voltages. The accuracy of our model will be established by experimental measurement of cytoplasmic Ca concentration or of the Ca conductance of the cGMP channels. If the Ca conductance at depolarized voltages were, in fact, small, the model would fail to predict the kinetics of DVAC. In this case, the required quenching of cGMP synthesis could be obtained by coupling activation of PDE with lowering cytoplasmic Ca. The success of the model suggests that in cone outer segments the velocity of guanylate cyclase activity is limited by the rate of change in cytoplasmic Ca concentration. The dependence of the enzyme on Ca concentration in the cones is indistinguishable from that described for rods.

APPENDIX

Calculation of Voltage- and Time-dependent Changes in Cytoplasmic Ca Concentration

To calculate cytoplasmic Ca concentration in the cone outer segment we follow the formalism of Sneyd and Tranchina (1989). We assume that the total internal Ca concentration, $[Ca]_T$, is determined from the kinetic balance between its influx through the cGMP-gated channels and its efflux through the Na/Ca,K exchanger (Yau and Nakatani, 1985; Miller and Korenbrot, 1987), and that the free Ca concentration, $[Ca]_i$, is a small fraction of the total Ca, $[Ca]_T$, because of the presence of Ca buffering in the outer segment. Ω is a measure of the Ca buffering power.

$$[Ca]_T = \Omega[Ca]_i \tag{A1}$$

Ca ions permeate through the light-sensitive, cGMP-gated channels of the cone outer segment (Perry and McNaughton, 1991); however, the voltage dependence of this conductance is unknown. The Ca current (in amperes), I_{Ca}, is given by the Ca-specific conductance of the cGMP-gated channels times the electromotive driving force for Ca. By convention, we assigned inward current a negative sign:

$$I_{Ca} = g_v (V - V_{eq}) \tag{A2}$$

g_v is the Ca conductance at voltage V and V_{eq} is the equilibrium potential for Ca across the outer segment membrane (in our case $+103$ mV, as given by the Nernst equation and the Ca concentrations inside [270 nM] and outside [1 mM] the cell).

From the current, Ca influx (in units of molar per second), J_{in}, was calculated:

$$J_{in} = \frac{I_{Ca}}{2F} \tag{A3}$$

where F is Faraday's constant. The component of the rate of change in cytoplasmic Ca due to influx through the cGMP-gated channels is given by:

$$\frac{d[Ca]_i^{Jin}}{dt} = \alpha_0 I_{Ca} \tag{A4}$$

where

$$\alpha_0 = \frac{1}{2v\Omega F} \tag{A5}$$

and v is the volume of the cone outer segment.

Ca efflux occurs through the Na/Ca,K exchanger and its magnitude is determined by the

cytoplasmic Ca concentration and a transport rate that reflects the molecular properties of the exchanger (Miller and Korenbrot, 1987; Lagnado and McNaughton, 1990). Ca efflux (in units of molar per second), J_{eff}, was calculated thus:

$$J_{eff} = \beta[Ca]_i \qquad (A6)$$

where β is a transport constant that has units of volume/time and is equal to the volume of the cone outer segment divided by the time constant of clearance of Ca from the outer segment.

The component of the rate of change in cytoplasmic Ca due to efflux through the Na/Ca,K exchanger is given by:

$$\frac{d[Ca]_i^{J_{eff}}}{dt} = \alpha_1\beta_1[Ca]_i \qquad (A7)$$

where

$$\alpha_1 = \frac{1}{v} \qquad \beta_1 = \frac{\beta}{\Omega}$$

The time constant of Ca clearance can be measured from the exponential decline in the electrogenic current of the exchanger measured when all influx is suddenly stopped by a bright flash of light, τ_{ex} (Nakatani and Yau, 1989; Hestrin and Korenbrot, 1990; Perry and McNaughton, 1991). In single bass cones we determined that at -40 mV the average value of τ_{ex} was 111 ms ($\pm 11.3 \pm$ SD; $n = 5$).

These relations were used to estimate changes in cytoplasmic Ca upon depolarization from a holding voltage of -40 mV (V_h) to some command voltage (V_{comm}). To execute these calculations, we defined the net rate of change in Ca concentration to be the algebraic sum of the rate of change of $[Ca]_i$ due to influx through the cGMP-gated channels and the rate of change of $[Ca]_i$ due to efflux through the exchanger.

$$\frac{d}{dt}[Ca]_i = \frac{d}{dt}[Ca]_i^{J_{in}} - \frac{d}{dt}[Ca]_i^{J_{eff}} \qquad (A8)$$

We estimated the Ca inward current at each voltage as follows. The amplitude of the electrogenic Na/Ca,K exchanger current measured under voltage clamp when outer segment current is suppressed by bright light is a measure of the Ca flux through the cGMP-gated channels at the holding voltage (Hestrin and Korenbrot, 1990; Perry and McNaughton, 1991). In striped bass single cones held at -40 mV, this component has an average value of 7% of the saturated photocurrent amplitude ($\pm 1.1\%$; $n = 5$), a value similar to that reported for tiger salamander single cones (6%: Hestrin and Korenbrot, 1990; 10%: Perry and McNaughton, 1991). For each cell studied, we measured its saturated photocurrent amplitude and estimated the Ca influx at -40 mV to be 7% of that number. From Eq. A2 we could estimate the Ca conductance at holding voltage, g_{V_h}. The average value of g_{V_h} was 12.6×10^{-12} S ($\pm 2.98 \times 10^{-12}$ SD; $n = 8$). Since the voltage dependence of Ca conductance in the cGMP-gated channels is unknown, we defined an adjustable parameter, $\gamma_{V_{comm}}$, at each command voltage:

$$\gamma_{V_{comm}} = \frac{g_{V_{comm}}}{g_{V_h}} \qquad (A9)$$

where $g_{V_{comm}}$ is the Ca conductance at command voltage, V_{comm}. We interpret $\gamma_{V_{comm}}$ as the Ca conductance of the cGMP-dependent current at each voltage as a fraction of the conductance at the holding voltage.

Thus, we calculated the voltage- and time-dependent Ca current at V_{comm}:

$$I_{Ca}(V_{comm}, t) = \gamma_{V_{comm}} g_{V_h} \epsilon(t)(V_{comm} - V_{eq}) \tag{A10}$$

where $\epsilon(t)$ is the time course and amplitude of the conductance enhancement. In simulations, the experimentally measured conductance enhancement for each cell was provided as data to define this parameter.

Changes in current were converted to changes in Ca flux (Eq. A3) and used to solve Eq. A8. To determine the cytoplasmic Ca concentration, without independently knowing the value of Ω, we assigned an initial condition at the holding voltage with $[Ca]_{iV_h}$ equal to 270 nM. This
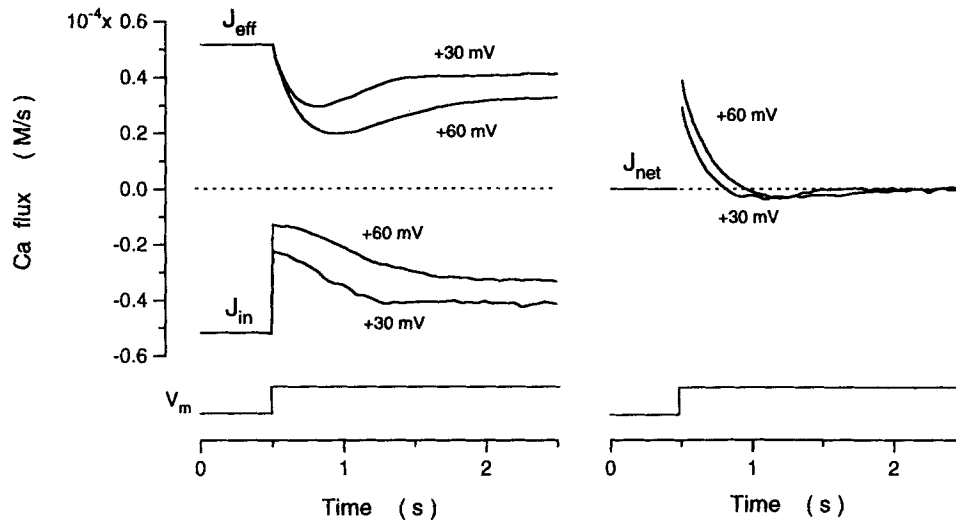

FIGURE 9.   Simulations of changes in Ca fluxes across the cone outer segment membrane in response to membrane depolarization from −40 mV holding potential to +30 mV or +60 mV. Illustrated are the time course of changes in Ca influx, efflux, and net flux calculated as detailed in the Appendix. By convention, inward flux is shown as negative. The data shown are taken from successful fits to experimental results. The panels on the left illustrate the Ca influx (J_{in}) and efflux (J_{eff}). The panel on the right illustrates the net Ca flux, the algebraic sum of influx, and efflux (J_{net}). At the holding voltage, influx and efflux are the same and the net flux is zero. Upon depolarization the influx decreases initially as the membrane potential approaches the equilibrium potential for Ca ions, but then increases again as the membrane conductance is enhanced. Upon depolarization, the net flux is initially outward (positive), but then becomes inward before becoming zero again when the influx and efflux regain steady state.

number is based on direct measurements of dark $[Ca]_i$ in rod outer segments (Ratto et al., 1988; Korenbrot and Miller, 1989). In the simulations, we adjusted the value of Ω to best-fit experimental data. In a sense, in the simulations the activity of the guanylate cyclase acted as a reporter of cytoplasmic Ca concentration.

Fig. 9 illustrates the results of simulations of Ca influx, Ca efflux, and net Ca flux carried out with the model described above. The data shown are those calculated in a simulation that fit experimental data. Average values of the adjustable parameters are presented in Table I. As expected, depolarization causes a rapid, initial decrease in Ca influx since the driving force is decreased; as the underlying conductance increases, Ca influx recovers to a final steady state.

The Ca efflux decreased initially but it then increased again as Ca "flooded" the outer segment through the enhanced conductance. In response to the command voltage, the net flux is initially outward and then becomes inward as Ca enters through the enhanced conductance. In the steady state at V command, again, net Ca flux is zero.

REFERENCES

Attwell, D., F. S. Werblin, and M. Wilson. 1982. The properties of single cones isolated from the tiger salamander retina. *Journal of Physiology.* 328:259–283.

Barkdoll, A. E., III, E. N. Pugh, Jr., and A. Sitaramayya. 1989. Calcium dependence of activation and inactivation kinetics of the light-activated phosphodiesterase of retinal rods. *Journal of General Physiology.* 93:1091–1108.

Barnes, S., and B. Hille. 1989. Ionic channels of the inner segment of tiger salamander cone photoreceptors. *Journal of General Physiology.* 94:719–744.

Baylor, D. A. 1987. Photoreceptor signals and vision. *Investigative Ophthalmology & Visual Science.* 28:34–49.

Baylor, D. A., A. L. Hodgkin, and T. D. Lamb. 1974. The electrical response of turtle cones to flashes and steps of light. *Journal of Physiology.* 242:685–727.

Baylor, D. A., T. D. Lamb, and K.-W. Yau. 1979. The membrane current of single rod outer segments. *Journal of Physiology.* 288:589–611.

Baylor, D. A., and B. J. Nunn. 1986. Electrical properties of the light-sensitive conductance of rods of the salamander Ambystoma tigrinum. *Journal of Physiology.* 371:115–145.

Cherr, G. N., and N. L. Cross. 1987. Immobilization of mammalian eggs on solid substrates by lectins for electron microscopy. *Journal of Microscopy.* 145:341–345.

Cobbs, W. H., A. E. Barkdoll III, and E. N. Pugh, Jr. 1985. Cyclic GMP increases photocurrent and light sensitivity of retinal cones. *Nature.* 317:64–66.

Del Priore, L. V., and A. Lewis. 1983. Calcium-dependent activation and deactivation of rods outer segment phosphodiesterase is calmodulin-independent. *Biochemical and Biophysical Research Communications.* 113:317–324.

Dizhoor, A. M., S. Ray, S. Kumar, G. Niemi, M. Brolley, D. Spencer, K. A. Walsh, P. P. Philipov, J. B. Hurley, and L. Stryer. 1991. Recoverin: a calcium sensitive activator of retinal rod guanylate cyclase. *Science.* 251:915–918.

Fain, G. L., T. D. Lamb, H. R. Matthews, and R. L. W. Murphy. 1989. Cytoplasmic calcium as the messenger for light-adaptation in salamander rods. *Journal of Physiology.* 416:215–243.

Fleischman, D., and M. Denisevich. 1979. Guanylate cyclase of isolated bovine retinal rod axonemes. *Biochemistry.* 18:5060–5066.

Gillespie, P. G., and J. A. Beavo. 1988. Characterization of a bovine cone photoreceptor phosphodiesterase purified by cyclic GMP-sepharose chromatography. *Journal of Biological Chemistry.* 263:8133–8141.

Goldberg, N. D., A. Ames III, J. E. Gander, and T. F. Walseth. 1983. Magnitude of increase in retinal cGMP metabolic flux determined by ^{18}O incorporation into nucleotide α-phosphoryls corresponds with intensity of photic stimulation. *Journal of Biological Chemistry.* 258:9213–9219.

Hamill, O. P., A. Marty, E. Neher, B. Sakmann, and F. J. Sigworth. 1981. Improved patch-clamp techniques for high-resolution current recording from cells and cell-free membrane patches. *Pflügers Archiv.* 391:85–100.

Haynes, L. W., and K. W. Yau. 1985. Cyclic GMP-sensitive conductance in outer segment membrane of catfish cones. *Nature.* 317:61–64.

Haynes, L. W., and K.-W. Yau. 1990. Single-channel measurements from the cGMP-activated conductance of catfish retinal cones. *Journal of Physiology.* 429:451–481.

Hestrin, S., and J. I. Korenbrot. 1987. Effects of cyclic GMP on the kinetics of the photocurrent in rods and detached rod outer segments. *Journal of General Physiology.* 90:527–551.

Hestrin, S., and J. I. Korenbrot. 1990. Activation kinetics of retinal cones and rods: response to intense flashes of light. *Journal of Neuroscience.* 10:1967–1973.

Hodgkin, A. L., and B. J. Nunn. 1988. Control of light-sensitive current in salamander rods. *Journal of Physiology.* 403:439–471.

Hurwitz, R. L., A. H. Bunt-Milam, M. L. Change, and J. A. Beavo. 1985. cGMP phosphodiesterase in rod and cone outer segments of the retina. *Journal of Biological Chemistry.* 260:568–573.

Kawamura, S., and M. D. Bownds. 1981. Light adaptation of the cyclic GMP phosphodiesterase of frog photoreceptor membranes mediated by ATP and calcium ions. *Journal of General Physiology.* 77:571–591.

Kawamura, S., and M. Murakami. 1989. Regulation of cGMP levels by guanylate cyclase in truncated frog rod outer segments. *Journal of General Physiology.* 94:649–668.

Kawamura, S., and M. Murakami. 1991. Calcium-dependent regulation of cyclic GMP phosphodiesterase by a protein from frog retinal rods. *Nature.* 349:420–423.

Koch, K. W., F. Eckstein, and L. Stryer. 1990. Stereochemical course of the reaction catalyzed by guanylate cyclase from bovine retinal rod outer segments. *Journal of Biological Chemistry.* 265:9659–9663.

Koch, K. W., and L. Stryer. 1988. Highly cooperative feed-back control of retinal rod guanylate cyclase by calcium ion. *Nature.* 334:64–66.

Korenbrot, J. I., and A. V. Maricq. 1991. Calcium channels in sensory transduction: a case study in photoreceptors. *In* Calcium Channels: Their properties, Functions, Regulation and Clinical Relevance. L. Hurwitz, L. D. Partdridge, and J. K. Leach, editors. CRC Press, Inc., Boca Raton, FL. 107–124.

Korenbrot, J. I., and D. L. Miller. 1986. Calcium ions act as modulators of intracellular information flow in retinal rod phototransduction. *Neuroscience Research.* 4:S11–S34.

Korenbrot, J. I., and D. L. Miller. 1989. Cytoplasmic free calcium concentration in dark-adapted retinal rod outer segments. *Vision Research.* 29:939–948.

Krishnan, N., R. T. Fleischer, G. J. Chader, and G. Krishna. 1978. Characterization of guanylate cyclase of rod outer segments of the bovine retina. *Biochimica et Biophysica Acta.* 523:506–515.

Lagnado, L., and P. A. McNaughton. 1990. Electrogenic properties of the Na:Ca exchange. *Journal of Membrane Biology.* 113:177–191.

Lambrecht, H.-G., and K.-W. Koch. 1991. A 26 kd calcium binding protein from bovine rod outer segment as modulator of photoreceptor guanylate cyclase. *EMBO Journal.* 10:793–798.

Liebman, P. A., K. R. Parker, and E. A. Dratz. 1987. The molecular mechanism of visual excitation and its relation to the structure and composition of the rod outer segment. *Annual Review of Physiology.* 49:765–791.

Lolley, R. N., and E. Racz. 1982. Calcium modulation of cyclic GMP synthesis in rat visual cells. *Vision Research.* 22:1481–1486.

Maricq, A. V., and J. I. Korenbrot. 1988. Calcium and calcium-dependent chloride currents generate action potentials in solitary cone photoreceptors. *Neuron.* 1:503–515.

Maricq, A. V., and J. I. Korenbrot. 1990a. Inward rectification in the inner segment of single retinal cone photoreceptors. *Journal of Neurophysiology.* 64:1917–1928.

Maricq, A. V., and J. I. Korenbrot. 1990b. Potassium currents in the inner segment of single retinal cone photoreceptors. *Journal of Neurophysiology.* 64:1929–1940.

Matthews, H. R. 1991. Incorporation of chelator into guinea-pig rod shows that calcium mediates mammalian photoreceptor light adaptation. *Journal of Physiology.* 436:93–105.

Matthews, H. R., G. L. Fain, R. L. W. Murphy, and T. D. Lamb. 1990. Light adaptation in cones of the salamander: a role for cytoplasmic calcium concentration. *Journal of Physiology.* 420:447–469.

McNaughton, P. A. 1990. Light response of vertebrate photoreceptors. *Physiological Reviews.* 70:847–883.

McNaughton, P. A., L. Cervetto, and B. J. Nunn. 1986. Measurement of the intracellular free calcium concentration in salamander rods. *Nature.* 322:261–263.

Miller, D. L., and J. I. Korenbrot. 1987. Kinetics of light-dependent Ca fluxes across the plasma membrane of rod outer segments. A dynamic model of the regulation of cytoplasmic Ca concentration. *Journal of General Physiology.* 90:397–426.

Nakatani, K., and K.-W. Yau. 1988. Calcium and light adaptation in retinal rods and cones. *Nature.* 334:69–71.

Nakatani, K., and K.-W. Yau. 1989. Sodium-dependent calcium extrusion and sensitivity regulation in retinal cones of the salamander. *Journal of Physiology.* 409:525–548.

Orlov, N. Y., E. V. Kalinin, T. G. Orlova, and A. A. Freidin. 1988. Properties and content of cyclic nucleotide phosphodiesterase in photoreceptor outer segments of ground squirrel retina. *Biochimica et Biophysica Acta.* 954:325–335.

Pepe, I. M., A. Boero, L. Vergani, I. Panfoli, and C. Cugnoli. 1986. Effect of light and calcium on cyclic GMP synthesis in rod outer segments of toad retina. *Biochimica et Biophysica Acta.* 889:271–276.

Perry, R. J., and P. A. McNaughton. 1991. Response properties of cones from the retina of the tiger salamander. *Journal of Physiology.* 433:561–587.

Picones, A., and J. I. Korenbrot. 1992. Permeation and interaction of monovalent cations with the cGMP-gated channel of cone photoreceptors. *Journal of General Physiology.* 100:647–674.

Pugh, E. N., Jr., and W. H. Cobbs. 1986. Visual transduction in vertebrate rods and cones: a tale of two transmitters, calcium and cyclic GMP. *Vision Research.* 26:1613–1643.

Pugh, E. N., Jr., and T. D. Lamb. 1990. Cyclic GMP and calcium: the internal messengers of excitation and adaptation in vertebrate photoreceptors. *Vision Research.* 30:1923–1948.

Ratto, G. M., R. Payne, R. G. Owen, and R. Y. Tsien. 1988. The concentration of cytosolic free calcium in vertebrate rod outer segment measured with Fura-2. *Journal of Neuroscience.* 8:3240–3246.

Rispoli, G., and P. B. Detwiler. 1991. Voltage-dependence of light-sensitive and Na/Ca exchange currents in detached lizard retinal rod outer segments. *Biophysical Journal.* 59:534a. (Abstr.)

Robinson, P. R., S. Kawamura, B. Abramson, and M. D. Bownds. 1980. Control of the cyclic GMP phosphodiesterase of frog photoreceptor membranes. *Journal of General Physiology.* 76:631–645.

Sather, W. A., and P. B. Detwiler. 1987. Intracellular biochemical manipulation of phototransduction in detached rod outer segments. *Proceedings of the National Academy of Sciences, USA.* 84:9290–9294.

Sneyd, J., and D. Tranchina. 1989. Phototransduction in cones: an inverse problem in enzyme kinetics. *Bulletin of Mathematical Biology.* 51:749–784.

Torre, V., H. R. Matthews, and T. D. Lamb. 1986. The role of calcium in regulating the cyclic GMP cascade of phototransduction in retinal rods. *Proceedings of the National Academy of Sciences, USA.* 83:7109–7113.

Tranchina, D., J. Sneyd, and I. D. Cadenas. 1991. Light-adaptation in turtle cones. testing and analysis of a model for phototransduction. *Biophysical Journal.* 60:217–237.

Yau, K.-W., and D. A. Baylor. 1989. Cyclic GMP-activated conductance of retinal photoreceptor cells. *Annual Review of Neuroscience.* 12:289–327.

Yau, K.-W., and K. Nakatani. 1985. Light-induced reduction of cytoplasmic free calcium in retinal rod outer segment. *Nature.* 313:579–582.